THE JOURNAL OF BIOLOGICAL CHEMISTRY
Vol. 273, No. 25, Issue of June 19, pp. 15559–15564, 1998

Printed in U.S.A.

Isolation and Characterization of PDE9A, a Novel Human cGMP-specific Phosphodiesterase*

(Received for publication, December 22, 1997, and in revised form, April 1, 1998)

Douglas A. Fisher‡§, James F. Smith‡, Joann S. Pillar¶, Suzanne H. St. Denis‡, and John B. Cheng¶

From the ‡Department of Molecular Sciences and the ¶Department of Cancer, Immunology and Infectious Diseases, Pfizer Central Research, Groton, Connecticut 06340

We have cloned and characterized the first human isozyme in a new family of cyclic nucleotide phosphodiesterases, PDE9A. By sequence homology in the catalytic domain, PDE9A is almost equidistant from all eight known mammalian PDE families but is most similar to PDE8A (34% amino acid identity) and least like PDE5A (28% amino acid identity). We report the cloning of human cDNA encoding a full-length protein of 593 amino acids, including a 261-amino acid region located near the C terminus that is homologous to the ~270-amino acid catalytic domain of other PDEs. PDE9A is expressed in all eight tissues examined as a ~2.0-kilobase mRNA, with highest levels in spleen, small intestine, and brain. The full-length PDE9A was expressed in baculovirus fused to an N-terminal 9-amino acid FLAG tag. Kinetic analysis of the baculovirus-expressed enzyme shows it to be a very high affinity cGMP-specific PDE with a K_m of 170 nM for cGMP and 230 μM for cAMP. The K_m for cGMP makes PDE9A one of the highest affinity PDEs known. The V_{max} for cGMP (4.9 nmol/min/μg recombinant enzyme) is about twice as fast as that of PDE4 for cAMP. The enzyme is about twice as active *in vitro* in 1–10 mM Mn^{2+} than in the same concentration of Mg^{2+} or Ca^{2+}. PDE9A is insensitive (up to 100 μM) to a variety of PDE inhibitors including rolipram, vinpocetine, SKF-94120, dipyridamole, and 3-isobutyl-1-methyl-xanthine but is inhibited (IC_{50} = 35 μM) by zaprinast, a PDE5 inhibitor. PDE9A lacks a region homologous to the allosteric cGMP-binding regulatory regions found in the cGMP-binding PDEs: PDE2, PDE5, and PDE6.

Cyclic nucleotide phosphodiesterases (PDEs),[1] which hydrolyze the intracellular second messengers cAMP and cGMP to their corresponding monophosphates, play an important role in signal transduction by regulating the intracellular concentration of cyclic nucleotides. Eight families of mammalian PDEs have been defined based on sequence similarity, substrate specificity, affinity, sensitivity to cofactors, and sensitivity to inhibitory drugs (1).[2] These families are: PDE1, Ca^{2+}/calmodulin-dependent; PDE2, cGMP-stimulated; PDE3, cGMP-inhibited; PDE4, cAMP-specific; PDE5, cGMP-specific; PDE6, photoreceptor cGMP-specific; PDE7, cAMP-specific rolipram-insensitive; and PDE8, cAMP-specific IBMX-insensitive. Within families, there are multiple isozymes and multiple splice variants of those isozymes. PDEs are composed of a catalytic domain of ~270 amino acids, an N-terminal regulatory domain responsible for binding cofactors, and in some cases, a C-terminal domain of unknown function. Within the catalytic domain, there is approximately 30% amino acid identity between PDE families and ~85–95% identity between isozymes of the same family (*e.g.* PDE4A *versus* PDE4B). Furthermore, within a family there is extensive similarity (>60%) outside the catalytic domain, whereas across families there is little or no sequence similarity.

The existence of multiple PDE families, isozymes, and splice variants presents an opportunity for complex regulation of cyclic nucleotide levels. To better understand this regulation and to identify the molecules responsible, we have looked for novel cyclic nucleotide phosphodiesterases. In this study, we describe the cloning, tissue distribution, expression, and pharmacology of a new human high affinity cGMP-specific phosphodiesterase. Sequence comparisons with the published PDEs and its pharmacological properties show that this enzyme, PDE9A, defines a new family of cyclic nucleotide phosphodiesterase. The murine homologue of PDE9A has been simultaneously and independently cloned by others and is being submitted as a separate report (2).

EXPERIMENTAL PROCEDURES

All procedures not detailed below were performed as described by Sambrook *et al.* (3).

Isolation and Analysis of cDNA Sequences—One EST clone was identified by searching the Incyte EST data base (Incyte Pharmaceuticals Inc., Palo Alto, CA) using the Basic Local Alignment Search Tool (BLAST) (4). The sequence of human PDE4B (5, 6) was used as the query. Novel clones were sequenced using PCR-based fluorescent sequencing on an Applied Biosystems (Foster City, CA) model 373 sequencer.

Northern Blot Analysis—3 μg of human poly(A)$^+$ RNA (CLONTECH Laboratories, Inc., Palo Alto, CA) from eight tissues was electrophoresed through a 1% formaldehyde agarose denaturing gel, transferred to a nylon membrane (Hybond N+, Amersham Pharmacia Biotech), and hybridized with a ^{32}P-labeled probe composed of the 5′-most 1090 nucleotides of Incyte clone 828,228 (nucleotides 809–1899 in Fig. 2). Probe DNA was labeled with ^{32}P using the "Ready-To-Go" random prime labeling kit (Amersham Pharmacia Biotech) and washed to a stringency of 0.5 × SSC, 65 °C. For the mouse Northern blot, this probe was hybridized to a mouse multiple tissue Northern blot (CLONTECH) and washed to a stringency of 1 × SSC, 65 °C.

5′ Extension of ESTs—cDNA sequences were extended by PCR amplification from human λgt10 testis or stomach cDNA library DNA (CLONTECH) using nested primers. Briefly, 2.5 × 10^7 plaque-forming

* The costs of publication of this article were defrayed in part by the payment of page charges. This article must therefore be hereby marked "*advertisement*" in accordance with 18 U.S.C. Section 1734 solely to indicate this fact.

The nucleotide sequence(s) reported in this paper has been submitted to the GenBank™/EBI Data Bank with accession number(s) AF048837.

§ To whom correspondence should be addressed. Tel.: 860-441-6109; Fax: 860-441-3493; E-mail: douglas_a_fisher@groton.pfizer.com.

[1] The abbreviations used are: PDE, 3′:5′ cyclic nucleotide phosphodiesterase; PCR, polymerase chain reaction; EST, expressed sequence tag; kb, kilobase(s); IBMX, 3-isobutyl-1-methyl-xanthine; SKF-95120, 5-(4-acetamidophenyl) pyrazin-2-(1H)-one; RACE, rapid amplification of cDNA ends.

[2] Fisher, D. A., Smith, J. F., Pillar, J. S., St. Denis, S. H., and Cheng, J. B., (1998) *Biochem. Biophys. Res. Commun.* **246,** in press.

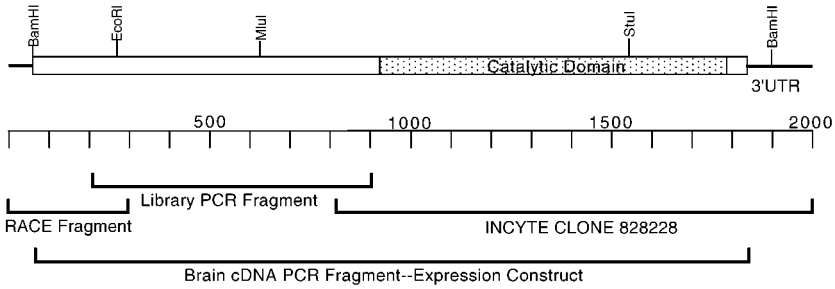

FIG. 1. **Clone map of PDE9A.** Coding regions are shown as *boxes*, and the catalytic domain is shown as a *shaded box*. The 5′- and 3′-untranslated regions (*UTR*) are denoted by a *line*. The scale is in nucleotides. The boundaries of Incyte clone 828,228 as well as the regions cloned by PCR are shown below the scale.

unit/reaction was boiled for 5 min to release DNA from the phage particles and chilled on ice. The first round of PCR (15 cycles) was performed with a PDE9A gene-specific primer (9A-specific outer: 5′-GACACAGAACAGCCACCTC-3′, nucleotides 966–950) and either a gt10 forward (5′-TCGCTTAGTTTTACCGTTTTC-3′ or a gt10 reverse (5′-TATCGCCTCCATCAACAAACTT-3′) primer. 1⁄50 of the reaction was used as template for a second round of PCR (30 cycles) with a nested PDE9A gene-specific primer (9A-specific inner: 5′-GGGTGACAGGGTTGATGCT-3′, nucleotides 945–927) with either a nested gt10 forward (5′-AGCAAGTTCAGCCTGGTTAAG-3′) or gt10 reverse (5′-CTTATGAGTATTTCTTCCAGGGTA-3′) primer. PCR primers were chosen (Oligo 5.0 primer analysis software, National Biosciences, Inc., Plymouth, MN) to be efficient at an annealing temperature of 55 °C. 5′ RACE (7) was performed to extend the sequence using human brain mRNA (CLONTECH) as template and the 5′ RACE System for Rapid Amplification of cDNA Ends kit (Life Technologies, Inc.) according to the manufacturer's protocol. PDE9A-specific primers used in the 5′ RACE were: reverse transcriptase primer, 5′-GCTCCTCCCTCATCTTCTTA-3′ (nucleotides 694–675); outer primer, 5′-AGGACAGCCAAGTGATTT-3′ (nucleotides 611–594); and inner primer, 5′-TGCGCTGGCCTTCCTGGTAG-3′ (nucleotides 493–474). All sequences that were subsequently incorporated into the PDE9A sequence were verified by sequencing multiple independent PCR amplification products from either cDNA library DNA or from brain cDNA using unique primers.

Expression of PDE9A in Insect Cells—A 1.8-kb region of PDE9A containing the full-length coding region (nucleotides 61–1842) was PCR amplified using the following primers: 5′ primer (nucleotides 8–25) = 5′-GCTGGCGTCGGGAAAGTA-3′ and 3′ primer (nucleotides 1825–1842) 5′-CGTCGACTTATTAGGCACAGTCTCCTTC-3′. The latter primer converts the TAG stop codon to a double TAA stop codon for more reliable termination and also adds a *Sal*I site at the 3′ end of the PCR fragment for cloning purposes. The fragment was subcloned into T-vector (Promega Biotech) and sequence verified, and the 1.8-kb *Bam*HI-*Sal*I fragment containing the full-length coding region was then cloned into the baculovirus transfer vector pFASTBAC (Life Technologies, Inc.), which had been modified to include a 5′ FLAG tag (8). The final N terminus of the recombinant protein is predicted to be MDYKDDDDKGSGSSSYR, where the underlined FLAG tag replaces the native start codon. Recombinant virus stocks were prepared according to the manufacturer's protocol. Sf9 cells were cultured in Sf900 II Sfm serum free medium (Life Technologies, Inc.) at 27 °C. For expression, 1×10^8 Sf9 cells were infected at a multiplicity of infection of 5 in a final volume of 50 ml. Two days post infection, the cells were harvested, and enzyme-containing lysates were prepared as detailed below under "Enzyme Preparation." To monitor expression, 1 μl of mock infected and PDE9A-infected lysate were electrophoresed in a polyacrylamide gel and either silver-stained by standard methods or transferred to nitrocellulose and Western blotted with an anti-FLAG antibody (M2, Scientific Imaging Systems, Eastman Kodak, New Haven, CT) at a concentration of 2 μg/ml. The secondary antibody was an alkaline phosphatase-conjugated anti-mouse IgG (Boehringer Mannheim), and the blot was visualized with a BCIP/NBT phosphatase substrate system (Kirkegaard & Perry Laboratories, Gaithersburg, MD) according to the manufacturer's protocol.

Enzyme Preparation—Transfected Sf9 cells were harvested by centrifugation, resuspended in homogenization buffer (20 mM Tris-HCl, 2 mM benzamidine, 1 mM EDTA, 0.25 M sucrose, 100 μM phenylmethylsulfonyl fluoride, pH 7.5) at 1×10^7 cells/ml and disrupted using a Branson sonicating probe (3×10 s pulses). Cellular debris was removed by centrifugation at $14{,}000 \times g$ for 10 min. The supernatant was stored at −70 °C until used.

Phosphodiesterase Assay—PDE activity was measured as described (9) with the following modifications: a one-step assay was run using a 100-μl assay volume containing 50 mM Tris-HCl, pH 7.5, 10 mM $MgCl_2$, 0.1 unit of 5′ nucleotidase (from *Crotalus atrox* venom), 0.064–0.1 μM [^{3}H]cGMP or [^{3}H]cAMP, and various concentrations of cold cyclic nucleotide to give the final concentration range for each: cGMP (0.064–2 μM) or cAMP (3–300 μM). The reaction was started by the addition of 25 μl of appropriately diluted enzyme supernatant. Reactions were run directly in mini Poly-Q scintillation vials (Beckman Instruments Inc., Fullerton, CA). Assays were incubated at 37 °C for a time period that would give less than 15% cGMP (or cAMP) hydrolysis to avoid nonlinearity associated with product inhibition. The reaction was stopped by the addition of 1 ml of Dowex AG1x8 (Cl form) resin (1:3 slurry). 3 ml of Ready Safe scintillant (Beckman) were added, and the vials were well mixed. The vials were allowed to settle for 1 h before counting. When inhibitors were tested, all reactions contained 1% Me_2SO and were done at a cGMP substrate concentration of 150 nM. The assay blank contained all reagents minus the enzyme aliquot. The level of PDE activity was so high in PDE9A-infected insect cells (≥ 200× higher than in mock infected cells) that the amount of basal insect cell cyclic nucleotide hydrolysis was considered negligible and ignored. At the dilutions used, the amount of cyclic nucleotide hydrolysis by the mock infected insect cell lysate was not significantly different from the no enzyme assay blank.

Source of PDE Inhibitors—Dipyridamole and IBMX were purchased from Sigma. SKF-94120 was a gift from the SmithKline & French Laboratories. Rolipram, zaprinast, and vinpocetin were synthesized at Pfizer Inc.

RESULTS

Cloning and Sequence Analysis of a Novel Human PDE—Bioinformatic screening of the Incyte data base yielded one EST clone homologous to the catalytic domain of PDE4B that was not identical to any known PDE. The identified clone, Incyte 828,228 (Fig. 1), was isolated from a prostate cDNA library. The clone sequence was extended in the 5′ direction using nested PCR from a testis cDNA library. This approach gave a 700-nucleotide PCR fragment that extended the sequence 600 nucleotides in the 5′ direction (Fig. 1) but did not give a full-length sequence. 5′ RACE from brain cDNA yielded fragments terminating at the beginning of the sequence shown in Fig. 2. To verify that the putative coding region (nucleotides 61–1842) is expressed as a contiguous fragment and to make an expression construct, this region was PCR amplified from human brain (medulla) cDNA and sequence verified.

Assembly of the clone and PCR sequences gives the 1991-nucleotide cDNA sequence shown in Fig. 2. The first 1839 nucleotides of this sequence contains an open reading frame that could encode a 613-amino acid polypeptide. However, as discussed below, it appears that the first methionine codon (beginning at nucleotide 61) is a natural start codon, making the PDE9A cDNA encode a full-length protein of 593 amino acids. This sequence includes a 261-amino acid region near its C terminus (amino acids 288–548, *underlined* in Fig. 2) with homology to the ~270-amino acid catalytic domain of cyclic nucleotide phosphodiesterases (Fig. 3). The rank order of similarity of this region to the other eight PDE families is as follows (% amino acid identity): PDE8A (34.4%), PDE7 (31.7%), PDE4 (31.3%), PDE1 (31.3%), PDE3 (30.1%), PDE2 (29.8%), PDE6 (28.9%), and PDE5 (27.8%). This level of similarity is the same as that seen between the catalytic domains of the eight

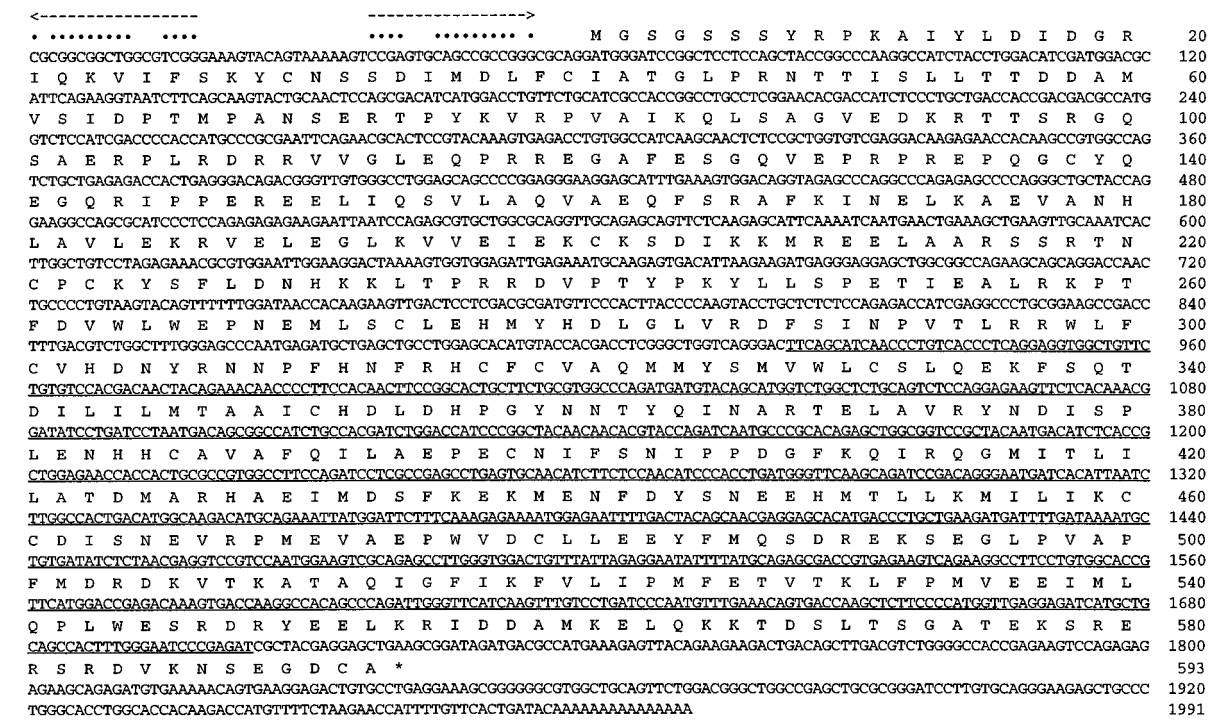

FIG. 2. **Nucleotide and protein sequence of PDE9A.** The protein sequence is shown as the single-letter code above the sequence. Nucleotide and protein numbering is indicated to the *right*. The nucleotide sequence of the catalytic domain is *underlined*. The location of an imperfect 18-nucleotide palindrome in the 5′-untranslated region is indicated by *two arrows*, and the nucleotides capable of base pairing are indicated by *dots*.

known PDE families and does not approach the >85% similarity seen between isozymes of the same family (*e.g.* 92% between PDE4A and PDE4B). Outside the catalytic domain, there is little or no sequence similarity with any other known PDE. Therefore, by sequence homology, this sequence represents a new family of PDE, which we denote as hsPDE9A2 in accordance with the nomenclature of the 1994 American Society of Pharmacology and Experimental Therapeutics Conference (10). The human cDNA is noted as the second splice variant of PDE9A to distinguish it from a different splice variant seen in the murine homologue of PDE9A (mmPDE9A1), described in the accompanying paper (2).

Fig. 3 shows an alignment of the catalytic domain of PDE9A with members of the other eight known mammalian PDE families. The clustering of sequence identity seen between the other eight PDE families also occurs in PDE9A. For example, of 22 amino acids conserved among all eight other PDE families, 21 are also conserved in PDE9A. The one change is a very conservative Tyr to Phe change at amino acid 24 of the catalytic domain (amino acid 311 in Fig. 2). Two divalent cation-binding motifs ($HisXaa_3HisXaa_{24-26}Glu$) thought to be critical to the catalytic activity of PDEs (11, 12) are conserved in PDE9A, with the exception that the glutamic acid of the first motif has been changed to aspartic acid (amino acid 341), another conservative change that is allowed in at least two other functional enzymes, PDE7A and PDE8A. All the features noted above are also conserved in the murine PDE9A sequence, which shares 93.5% amino acid sequence identity with the human sequence in the catalytic domain (2).

Tissue Distribution of PDE9A—Northern blot analysis with a PDE9A probe gives a single band of ~2.0 kb that is most abundant in spleen, small intestine, and brain mRNA (Fig. 4). However, the same sized mRNA is seen in all tissues examined to date, suggesting that PDE9A is broadly expressed. It remains to be shown if the quantitative differences between tissues will prove to be of any functional significance.

We have also confirmed that human PDE9A cross-hybridizes with murine PDE9A. The human PDE9A probe also detects only a 2.0-kb mRNA in a Northern blot of eight mouse tissues (data not shown). This is the same result seen with a mouse probe against a mouse Northern blot in the accompanying paper (2).

Expression of PDE9A in Insect Cells—Full-length PDE9A (amino acids 2–593) was expressed in insect cells with a 9-amino acid N-terminal FLAG tag (8) to assist in detection. Lysates made from infected Sf9 cells showed a new band with an apparent molecular mass of ~75 kDa by SDS-polyacrylamide gel electrophoresis (Fig. 5, *lanes 1* and *2*), which is in reasonable agreement with the 69.4-kDa molecular mass predicted for the FLAG-PDE9A fusion protein. Furthermore, this band comigrates with the only major protein that is positive in an anti-FLAG Western blot (Fig. 5, *lanes 3* and *4*). The amount of PDE9A expressed in the baculovirus lysate was estimated by comparison with a serial dilution of a known mass of bovine serum albumin on a silver-stained gel (data not shown). From this, we estimate the amount of PDE9A expressed to be 70 $\mu g/10^7$ infected Sf9 cells.

Kinetic Analysis of PDE9A—Recombinant PDE9A was identified as a catalytically active protein in that lysates from PDE9A-infected Sf9 cells expressed 200-fold greater cGMP hydrolyzing activity than mock infected cells. Further, this activity could be immunoprecipitated with anti-FLAG antibody-coated beads, indicating that the cGMP hydrolyzing activity was specifically associated with the FLAG-PDE9A fusion protein.

To determine the K_m and V_{max} of the enzyme, the rate of hydrolysis of cGMP and cAMP was measured at a variety of substrate concentrations using a very dilute enzyme preparation. Fig. 6 shows a Lineweaver-Burk plot of cGMP hydrolysis by PDE9A (13). The enzymatic activity of the baculovirus-expressed enzyme displayed standard Michaelis-Menten kinetics ($r^2 = 0.95$) with a K_m of 170 nM and a V_{max} of 4.9 nmol/min/μg of recombinant protein. Similar analysis reveals that the affinity for cAMP was >1000-fold lower, with a K_m of 230

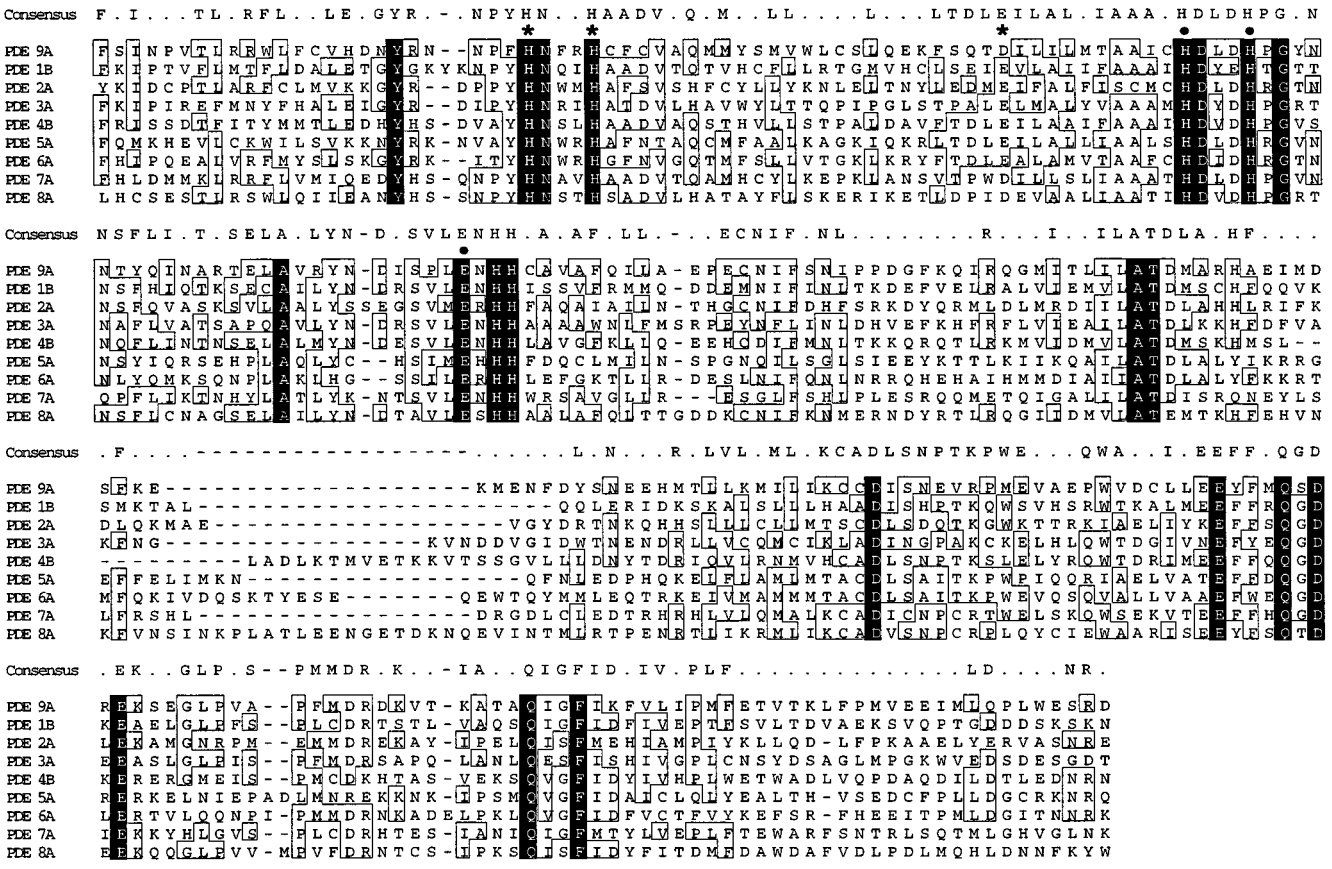

FIG. 3. **Alignment of the catalytic domain of PDE9A with mammalian PDEs.** A consensus sequence is shown above the alignment at those positions where at least 4 of the 9 sequences are identical, and those amino acids are *boxed* in the alignment. Positions where all 9 sequences are identical are noted with a *black box*. The location of the two divalent cation-binding motifs are indicated above the alignment as an *asterisk* or a *dot*. The mammalian PDE1–7 sequences are from published reports (6, 23–28). PDE8A is unpublished.[2] For clarity of alignment, a 44-amino acid insertion in PDE3A relative to the other PDEs has been deleted. This insertion occurs before the sequence PALELM (amino acids 51–56 in the PDE3A sequence).

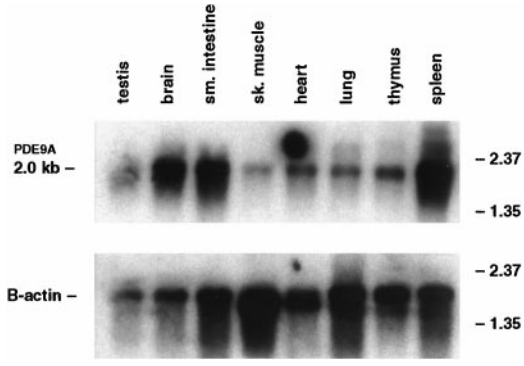

FIG. 4. **Tissue Northern blot of PDE9A.** Each lane contains 3 μg of human poly(A)$^+$ RNA from the indicated tissue. The sizes (in kilobases) and positions of mRNA size markers are shown to the right.

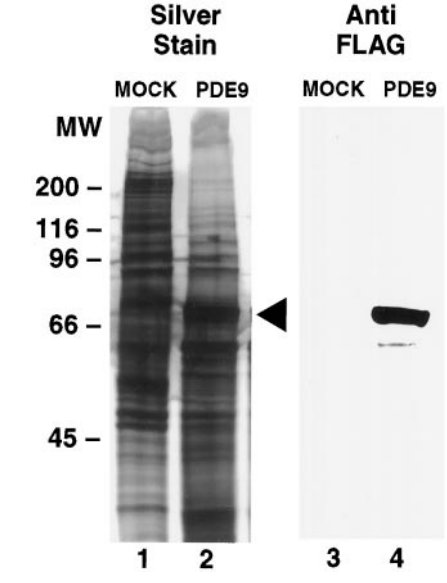

FIG. 5. **Insect cell expression of PDE9A.** The scale at left indicates the position of molecular mass (*MW*) markers. The *triangle* pointing to *lane 2* shows the position of a new silver-stained protein present in PDE9A containing baculovirus-infected Sf9 cells but not mock infected Sf9 cells. *Lanes 3* and *4* show an anti-FLAG Western blot of duplicates of *lanes 1* and *2*.

μM. To compare the activity of PDE9A with other known cAMP PDE enzymes, we expressed a human GST-PDE4A fusion protein and measured cAMP hydrolysis using identical expression and enzyme assay conditions. The PDE4A expressed in baculovirus showed a high affinity for cAMP with a K_m of 2.4 μM and a V_{max} of 2.2 nmol/min/μg of recombinant protein. Therefore, PDE9A has a 2-fold faster V_{max} for cGMP than that of PDE4A for cAMP.

PDE9A Activity Dependence on Cations/Inhibitor Studies—Like that of other PDEs, PDE9A activity is dependent on the presence of divalent cations, consistent with the role metal ions are thought to play in catalysis and the presence of conserved metal-binding sites in that catalytic domain (11, 12). Fig. 7 shows PDE9A activity at Mn^{2+}, Mg^{2+}, and Ca^{2+} concentrations from 100 μM to 100 mM. Maximal activity is achieved at Mn^{2+} concentrations of 1–10 mM, whereas Mg^{2+} or Ca^{2+} re-

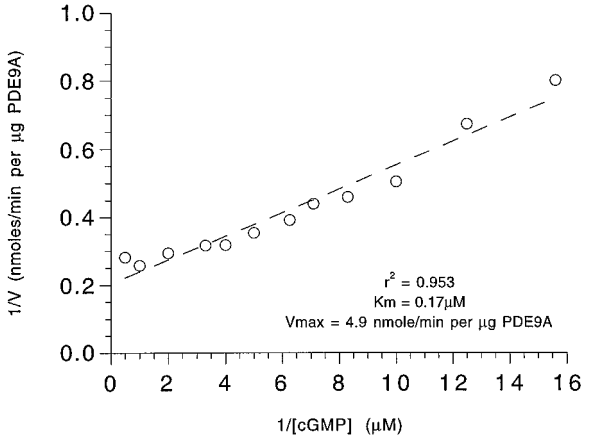

FIG. 6. **Lineweaver-Burk plot of PDE9A cGMP hydrolysis.** PDE activity was measured in a lysate of Sf9 cells that had been infected for 48 h. The cGMP concentration used in this experiment ranged from 0.064 to 2 μM. Enzyme concentration and incubation time were optimized to give no more than 15% cGMP conversion.

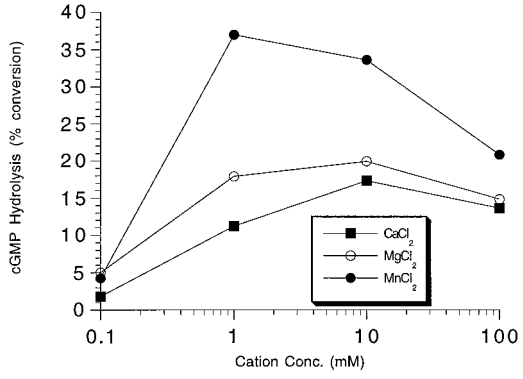

FIG. 7. **Dependence of PDE9A activity on divalent cation concentration.** The amount of enzyme and incubation time were optimized to give about 15% hydrolysis of cGMP under standard assay conditions (10 mM $MgCl_2$). cGMP concentration was 150 nM.

stores only ~50% of this activity.

To determine whether PDE8A activity is affected by any known PDE inhibitors, a dose-response curve against a panel of these agents was performed (Fig. 8). These inhibitors (PDEs that they inhibit in parenthesis) include rolipram (PDE4), SKF-94120 (PDE3), zaprinast (PDE5, 6), vinpocetine (PDE1), dipyridamole (PDE2, 4, 5, 6), and IBMX (nonspecific PDE). All the PDE inhibitors were inactive up to 100 μM with the exception of zaprinast, which had an IC_{50} of 35 μM.

DISCUSSION

The existence of multiple cyclic nucleotide phosphodiesterase families makes possible complex regulation of cyclic nucleotide levels. An elucidation of all such enzymes gives us tools to better understand cyclic nucleotide signal transduction, as well possible targets for pharmacological intervention once the biological relevance and any potential role in disease is established for each enzyme.

Human PDE9A represents the first human member of a new family of cGMP-specific PDE. Kinetic analysis shows PDE9A to be a very high affinity cGMP PDE with a 1000-fold higher affinity for cGMP (K_m = 170 nM) than for cAMP (K_m = 240 μM). Its lack of significant sequence homology with the eight other known mammalian PDE families outside the catalytic domain and 28–34% sequence identity within the catalytic domain is consistent with its assignment as a new family. Furthermore, PDE9A has an inhibitor profile unique among other known PDEs. Unlike the cGMP-binding PDEs (PDE2, PDE5, and

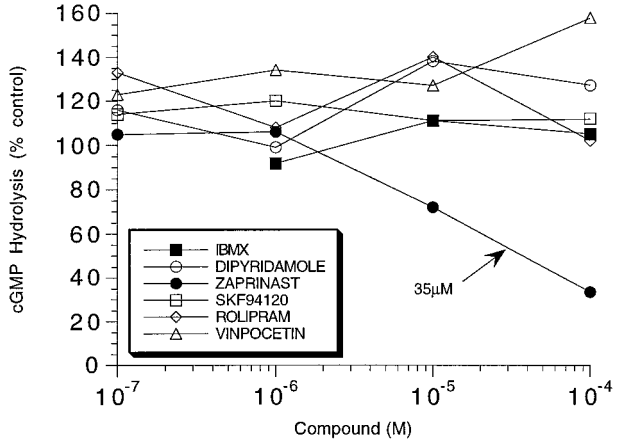

FIG. 8. **Effect of inhibitors on PDE9A.** Enzyme concentration and incubation time were optimized to give about 15% hydrolysis of cGMP in the absence of inhibitors, and this amount of conversion set to 100%. The cGMP concentration was 150 nM.

PDE6), the putative regulatory domain of PDE9A does not contain sequences homologous to the ~80-amino acid cGMP-binding regions that can serve as allosteric regulatory sites. Presumably, therefore, all binding of cGMP to PDE9A is at the catalytic site.

Among all previously published PDE sequences, PDE9A is most similar in the catalytic domain to a *D. discoideum* protein, RegA, that was identified genetically as a suppressor of an intracellular signaling defect (14). RegA has 40.6% amino acid identity with human PDE9A in the catalytic domain, which is greater than the 31–35% identity that RegA has with the other eight families of known mammalian PDEs. However, this similarity is far too low to consider PDE9A and RegA members of one PDE family. Consistent with this, PDE9A has little or no sequence similarity with RegA outside the catalytic domain. In addition, PDE9A and RegA are not functional homologues, because the two enzymes have very different properties: RegA is a cAMP-specific PDE with a K_m of 5 μM (15), whereas PDE9A is a much higher affinity cGMP-specific PDE.

A murine homologue of hsPDE9A2 with similar substrate specificity, kinetic properties, and inhibitor profile has been cloned simultaneously and is reported in the accompanying paper (2). The murine and human cDNAs share 93.5% amino acid identity in the catalytic domain. The primary difference between the sequences is the presence of 60 amino acids (amino acids 88–147 in Fig. 2) in the human PDE9A putative regulatory domain (amino acids 1–287) that are absent in the splice variant cloned in mouse. This suggests that alternate splicing of the putative regulatory domain is likely to occur in PDE9A, because it has been observed in other PDE families, where it can alter membrane targeting (16) and interaction with the v-Src SH3 domain (17). The PDE9A regulatory domain is otherwise 98% identical between the species, clearly indicating that these are two members of the same PDE family and almost certainly homologues of the same isozyme.

Analysis of the DNA sequence of PDE9A, including comparison with the murine sequence, indicates that we have obtained the coding sequence for a full-length 593-amino acid polypeptide. Both the human and mouse cDNAs predict the same start codon, which is flanked by sequences with a reasonable match for those found around eukaryotic initiator codons (18). Also, both cDNA sequences contain virtually all of the 2 kb mRNA seen in Northern blot experiments. Although there is only one amino acid substitution between species in the first 82 amino acids of these two polypeptides, all three amino acids predicted by the 9 known nucleotides upstream of the murine start codon

are different between the two species, indicating that this is untranslated region. This observation strengthens the assignment of this as the start codon in both species. Because the 15-nucleotide poly(A) sequence at the 3′ end of Incyte clone 828,228 is not preceded by a polyadenylation signal (19), it is that there could be a small amount of additional human 3′-untranslated region beyond that shown in Fig. 2.

It is worthwhile to point out that because alternatively spliced versions of human PDE9A probably exist, the molecular mass of PDE9A in any given tissue may not agree with that predicted from the sequence in Fig. 2. Although this sequence appears to be the most abundant form in human brain (medulla), further studies will be needed to correlate the specific molecular mass protein form expressed in various tissues.

The 5′-untranslated region of human PDE9A contains GC-rich sequences capable of folding back and forming a hairpin loop. The 18-nucleotide regions capable of base pairing are indicated in Fig. 2 with *arrows* to indicate their orientation and with *dots* to show the paired nucleotides. The central 9 of 9 nucleotide match is calculated to have a 49 °C melting temperature under physiological salt conditions (165 mM NaCl) (Oligo 5.0 primer analysis software, National Biosciences, Inc., Plymouth, MN). This raises the possibility that PDE9A protein expression may be at least partially regulated at the translational level, because the presence of hairpin structures in the 5′-untranslated region would be expected to inhibit translation. Ornithine decarboxylase, an enzyme involved in polyamine synthesis, is one example of an mRNA whose translation is profoundly affected by a hairpin structure in the 5′-untranslated region and whose translation efficiency is regulated by its enzymatic products (20). It remains to be shown whether the potential hairpin structure in the PDE9A 5′-untranslated region is biologically relevant.

The lack of PDE9A inhibition by most PDE inhibitors is not surprising given the low degree of sequence identity in the catalytic domain. Although the cGMP-binding pocket is probably highly conserved, there is already excellent precedent for family-specific inhibitors through examples such as rolipram. Rolipram inhibits PDE4 but not any other PDE family, including the other cAMP-specific PDEs, PDE7 and PDE8A. Pharmacological precedence and the large sequence differences between the catalytic domain of PDE9A and other known PDEs is highly favorable for efforts to find a PDE9A-selective inhibitor that would be valuable in exploring the biology of this enzyme.

The biological role of PDE9A is not presently known. Its broad tissue distribution does not suggest a role in a specific signal transduction pathway. The high affinity of PDE9A for cGMP, 20 and 100 times higher than that of PDE5 and PDE6, respectively (21, 22), suggests to us that PDE9A may be functioning in cells at lower cGMP concentrations than the other two cGMP PDEs. More detailed studies on the localization of PDE9A and studies with PDE9A-selective inhibitors may be informative in dissecting what cGMP-driven processes are regulated by this enzyme.

Acknowledgments—We are grateful to Alison Williams, Lisa Hayes, and Suzanne Williams of the DNA sequencing lab for expert technical assistance and to Katherine Cole and Dr. Steve Phillips for helpful comments on the manuscript. Thanks to Dr. Joe Beavo for sharing unpublished data and coordinating with us on the nomenclature of the human and mouse PDE9A and PDE8A gene families.

REFERENCES

1. Beavo, J. A. (1995) *Physiol. Rev.* **75,** 725–748
2. Soderling, S. H., Bayuga, S. J., and Beavo, J. A. (1998) *J. Biol. Chem.* **273,** 15553–15558
3. Sambrook, J., Fritsch, E. F., and Maniatis, T. (1989) *Molecular Cloning: A Laboratory Manual,* 2nd Ed., Cold Spring Harbor Laboratory, Cold Spring Harbor, NY
4. Altschul, S. F., Gish, W., Miller, W., Myers, E. W., and Lipman, D. J. (1990) *J. Mol. Biol.* **215,** 403–410
5. Bolger, G., Michaeli, T., Martins, T., St. John, T., Steiner, B., Rodgers, L., Riggs, M., Wigler, M., and Ferguson, K. (1993) *Mol. Cell. Biol.* **13,** 6558–6571
6. McLaughlin, M. M., Cieslinski, L. B., Burman, M., Torphy, T. J., and Livi, G. P. (1993) *J. Biol. Chem.* **268,** 6470–6476
7. Frohman, M. A., Dush, M. K., and Martin, G. R. (1988) *Proc. Natl. Acad. Sci. U. S. A.* **85,** 8998–9002
8. Kunz, D., Gerard, N. P., and Gerard, C. (1992) *J. Biol. Chem.* **267,** 9101–9106
9. Thompson, W. J., Brooker, G., and Appleman, M. M. (1974) *Methods Enzymol.* **38,** 205–212
10. Beavo, J. A., Conti, M., and Heaslip, R. J. (1994) *Mol. Pharmacol.* **46,** 399–405
11. Francis, S. H., Colbran, J. L., McAllister-Lucas, L. M., and Corbin, J. D. (1994) *J. Biol. Chem.* **269,** 22477–22480
12. Kleinman, E. F., Campbell, E., Giordano, L. A., Cohan, V. L., Jenkinson, T. H., Cheng, J. B., Shirley, J. T., Pettipher, E. R., Salter, E. D., Hibbs, T. A., DiCapua, F. M., and Border, J. (1998) *J. Med. Chem.* **41,** 266–270
13. Segel, I. H. (1976) *Biochemical Calculations*, 2nd Ed., pp. 233–236, John Wiley & Sons, New York
14. Shaulsky, G., Escalante, R., and Loomis, W. F. (1996) *Proc. Natl. Acad. Sci. U. S. A.* **93,** 15260–15265
15. Loomis, W. F., Shaulsky, G., and Wang, N. (1997) *J. Cell Sci.* **110,** 1141–1145
16. Shakur, Y., Pryde, J. G., and Houslay, M. D. (1993) *Biochem. J.* **292,** 677–686
17. O'Connell, J. C., McCallum, J. F., McPhee, I., Wakefield, J., Houslay, E. S., Wishart, W., Bolger, G., Frame, M., and Houslay, M. D. (1996) *Biochem. J.* **318,** 255–261
18. Kozak, M. (1987) *Nucleic Acids Res.* **15,** 8125–8148
19. Proudfoot, N. J., Cheng, C. C., and Brownlee, G. G. (1976) *Prog. Nucleic Acid Res. Mol. Biol.* **19,** 123–134
20. Grens, A., and Scheffler, I. E. (1990) *J. Biol. Chem.* **265,** 11810–11816
21. Francis, S. H., Lincoln, T. M., and Corbin, J. D. (1980) *J. Biol. Chem.* **255,** 620–626
22. Gillespie, P. G., and Beavo, J. A. (1988) *J. Biol. Chem.* **263,** 8133–8141
23. Bentley, J. K., Kadlecek, A., Sherbert, C. H., Seger, D., Sonnenburg, W. K., Charbonneau, H., Novack, J. P., and Beavo, J. A. (1992) *J. Biol. Chem.* **267,** 18676–18682
24. Trong, H. L., Beier, N., Sonnenburg, W. K., Stroop, S. D., Walsh, K. A., Beavo, J. A., and Charbonneau, H. (1990) *Biochemistry* **29,** 10280–10288
25. Meacci, E., Taira, M., Moos, M., Jr., Smith, C. J., Movsesian, M. A., Degerman, E., Belfrage, P., and Manganiello, V. (1992) *Proc. Natl. Acad. Sci. U. S. A.* **89,** 3721–3725
26. McAllister-Lucas, L. M., Sonnenburg, W. K., Kadlecek, A., Seger, D., Trong, H. L., Colbran, J. L., Thomas, M. K., Walsh, K. A., Francis, S. H., Corbin, J. D., and Beavo, J. A. (1993) *J. Biol. Chem.* **268,** 22863–22873
27. Pittler, S. J., Baehr, W., Wasmuth, J. J., McConnell, D. G., Champagne, M. S., vanTuinen, P., Ledbetter, D., and Davis, R. L. (1990) *Genomics* **6,** 272–283
28. Michaeli, T., Bloom, T. J., Martins, T., Loughney, K., Ferguson, K., Riggs, M., Rodgers, L., Beavo, J. A., and Wigler, M. (1993) *J. Biol. Chem.* **268,** 12925–12932